Available online at www.sciencedirect.com
ScienceDirect
Journal of Power Sources 163 (2007) 661–670
JOURNAL OF POWER SOURCES
www.elsevier.com/locate/jpowsour

The effect of composition of Ni-supported Pt-Ru binary anode catalysts on ethanol oxidation for fuel cells

Joyeeta Bagchi, Swapan Kumar Bhattacharya *

Physical Chemistry Section, Department of Chemistry, Jadavpur University, Kolkata 700032, India

Received 2 June 2006; received in revised form 3 August 2006; accepted 14 September 2006
Available online 13 November 2006

Abstract

The effect of the composition of a platinum-ruthenium (Pt-Ru) binary catalyst on a Ni-support for the anodic oxidation of ethanol in aqueous alkaline media has been studied. Co-deposition of nano-crystallites of a Pt-Ru electrocatalyst of varying composition, has been made on Ni-supports by galvanostatic deposition from precursor salt solutions of suitable composition, without using any capping agent. Conjugated scanning electron microscopic-energy dispersion X-ray spectroscopic studies reveal slight alteration of the atomic composition of the electrocatalyst on the electrode surface to that in the deposition bath, as expected. The excellent electrocatalytic activities of the electrodes for the anodic oxidation of ethanol have been found to depend on the mutual variation of composition of the binary catalyst. From cyclic voltammetric, chronopotentiometric, steady state polarization and electrochemical ac impedance studies, it can be inferred that the best catalytic activity of a Pt-Ru binary electrocatalyst on a Ni-support for anodic oxidation of ethanol contains 32–47 at.% of Ru. Moreover, the composition for the best activity within the said range is tilted towards more at.% of Ru when high current density is drawn whereas the composition containing a lower at.% of Ru is favoured when the current density drawn is relatively low.

Keywords: Ethanol electrooxidation; Electrocatalytic activity; Composition of binary catalyst; Electrochemical deposition of nano-particles; Best Pt-Ru composition

1. Introduction

During the last three decades [1–4], numerous studies have been made on platinum (Pt)-based binary metal electrocatalysts for the anodic oxidation of alcohols. In spite of such studies, a platinum-ruthenium (Pt-Ru) combination still remains the best choice [5,6] for both proton exchange membrane fuel cell (PEMFC) and direct alcohol fuel cell (DAFC), particularly at low temperatures. Consequently, studies [7–14] have also been devoted to defining the best composition of such binary anode-catalysts. Among them, some experimental findings [7–10] favour a low Ru-content, e.g., of about 20 at.% [7,8] or less [9,10], whereas many other studies on the anodic oxidation of methanol [6,11–13], CO [14], etc. reveal that the optimum atomic percentage for Ru is 50. Some researchers however give a range of 10–40 at.% Ru for good performance [15,16]. The different results have seemingly arisen due to the different methods of preparation of such electrodes, the difference in the surface and bulk compositions, the difference in precursor salts and the overall composition of the solution from which they had been prepared, as well as the variation in shape and size of the crystallites in different studies. Therefore, the problem of finding the best composition is still not fully solved and needs further studies. Notably, these investigations were done mainly with methanol. This is because methanol seems to be the most promising for its moderately high energy density (6 kWh kg^{-1}), greater solubility compared to hydrogen, availability at low cost, ease of storing, handling and transportation. Moreover, it is the simplest among the alcohols and thus its complete oxidation does not involve any C–C bond cleavage, as for higher alcohols. But methanol has some disadvantages. It has a low boiling (65 °C) point, is inflammable and is relatively toxic. It is not a primary or renewable fuel. So, we have witnessed increasing studies on other alcohols [1,17]. Among them, ethanol is thought to be the most outstanding because it is easily renewable by fermentation of raw materials received from agricultural sources and is thus cost-effective. But, until now only a few studies [1,6] have been performed to gather knowledge about the best composition of

* Corresponding author. Tel.: +91 98 31699643; fax: +91 33 24146584.
E-mail address: skbhatt7@yahoo.co.in (S.K. Bhattacharya).

0378-7753/$ – see front matter © 2006 Elsevier B.V. All rights reserved.
doi:10.1016/j.jpowsour.2006.09.063

the Pt-Ru electrode for ethanol oxidation. On the other hand, a decrease of Pt-loading in the construction of electrodes of a DAFC is always beneficiary for the reduction of the cost of the fuel cells. This helps to achieve market competitiveness for fuel cells with respect to available power generators. Thus such a study on the effect of change of % composition on the electrocatalytic capability of binary Pt-Ru anode for oxidation of ethanol is important. Moreover, from a purely thermodynamic point of view, the complete reaction for the anodic oxidation of ethanol as given by equation:

$$C_2H_5OH + 3H_2O = 2CO_2 + 12H^+ + 12e^- \quad (1)$$

which predicts that media with high pH make the reaction favourable, because alkali removes CO_2 and H_3O^+ from the system. For this, a highly negative value of the reversible and hence actual operating potential and hence a high practical efficiency [18,19] are achieved usually for fuel cells operating in alkaline media. There are other advantages too, for using alkali as the medium, e.g., less poisoning, less permeation of alcohol through the Nafion membrane, less depolarization of oxygen cathode, etc. These benefits have all been described elsewhere [5,20,21]. With this in view, we report in this paper the optimum at.% of Pt (and Ru) on a Ni-support, which can be used to prepare the best Pt-Ru electrode for a given set of conditions, for anodic oxidation of alcohols and particularly for ethanol in alkaline media. Techniques used in our work are cyclic voltammetry, chronopotentiometry (CP), galvanostatic polarization (GP), electrochemical impedance spectroscopy (EIS), scanning electron microscopy (SEM) and energy dispersion X-ray spectroscopy (EDX).

2. Experimental

2.1. Preparation of electrocatalysts

Ni-foil (>99.9% gold levels, Aldrich Chemical Company Inc.) having a thickness of 0.0125 cm was used as the support for the electrocatalyst. The middle portion of the foil was wrapped with Teflon tape (Champion), the lower portion was polished and degreased with distilled acetone and then dried. The upper portion of the foil was kept bare for electrical connection. Co-deposition of Pt-Ru on Ni-surface was done on the lower polished portion of the foil. The surface area of each of the electrodes was about 0.05 cm^2. As the shape and size of the crystallites of deposit may vary with rate of deposition, environmental solution composition and pH of solution of the deposition bath, method taken was such that they were kept constant during deposition. So, for the construction of Ni/Pt-Ru electrodes, cathodic co-deposition of Pt and Ru metals was performed on a Ni support at room temperature by applying a galvanostatic current density of 5 mA cm^{-2} for 30 min from different compositions of 2 wt% chloroplatinic acid ($H_2PtCl_6{\cdot}4H_2O$) and 2 wt% ruthenium chloride ($RuCl_3{\cdot}3H_2O$), both in 2 M HCl. Large platinum foil (1 cm × 1 cm) was used as a counter electrode for binary metal crystallization on Ni-support. The content of metal was 40 wt% for $H_2PtCl_6{\cdot}4H_2O$ and $RuCl_3{\cdot}3H_2O$ which were taken from Arora Matthey Ltd. and used as received. All the reagents used, were of AR grade and water used throughout the experiment was triply distilled. Current input during metal deposition, polarization and chronopotentiometric study were done by a constant current charger (DB-300, DB Electronics).

2.2. Electrochemical measurements

All electrochemical measurements were performed in a two-compartment glass-cell using a conventional three-electrode assembly. The reference electrode used was $Hg/HgO/OH^-$ (1 M) (MMO) whose equilibrium electrode potential was ~0.1 V with respect to standard hydrogen electrode (SHE). In all electrochemical measurements, a large Pt-foil (1 cm × 1 cm) was used as a counter electrode and all data of potential were recorded with respect to MMO. Cyclic voltammetric study was performed using a computer aided Potentiostat/Galvanostat (AEW-2, Munistst, Sycopel, Scientific Ltd., UK). Cyclic voltammograms (CV) of each electrode immersed in 1 M EtOH in 1 M NaOH were recorded during multiple scanning until a steady CV is obtained. Blank CVs were also taken in 1 M NaOH in absence of ethanol. Galvanostatic polarization and chronopotentiometry were performed with the help of a constant current charger (DB-300, DB Electronics and an EC digital multimeter DM 610 4B). Galvanostatic polarization was carried out by applying constant current density in the range of 0.2–3.2 mA cm^{-2}, for a long time until a steady potential is achieved. A change in potential of 1 mV or less in a time period of 10 min was considered as criterion of the steady state condition. The potential of all electrodes in steady state polarization and chronopotentiametric study, was noted by an EC digital multimeter DM 610B. The chronopotentiometric study was done by applying a current density of 0.4 mA cm^{-2}. For all measurements, the surface of the working electrodes was cleaned by keeping them in 1 M NaOH solution for 5 min at a constant potential of −900 mV, where hydrogen evolution occurred. Then the electrodes were taken in 1 M ethanol solution containing 1 M NaOH and allowed to equilibrate until a high negative value of steady open circuit potential is obtained/retained. Any further activation by sweep of potential or otherwise, was avoided to obviate any change of state of the surface of the electrodes before any electrochemical measurement, between 30 kHz and 30 mHz, after allowing equilibration of each electrode at the desired potential for 30 s. The measurement was conducted using a computer controlled potentiostat with PG STAT 12 and modules (Ecochemic BV, The Netherlands).

2.3. Surface studies

The morphology of the surfaces of the anodes was investigated with a JEOL-JSM-6360 scanning electron microscope (SEM) at an accelerating potential of 25 kV. The chemical composition of surfaces of catalysts was determined by energy dispersive X-ray (EDX) using INCAX-Stream Oxford instruments (UK) coupled with the scanning electron microscope.

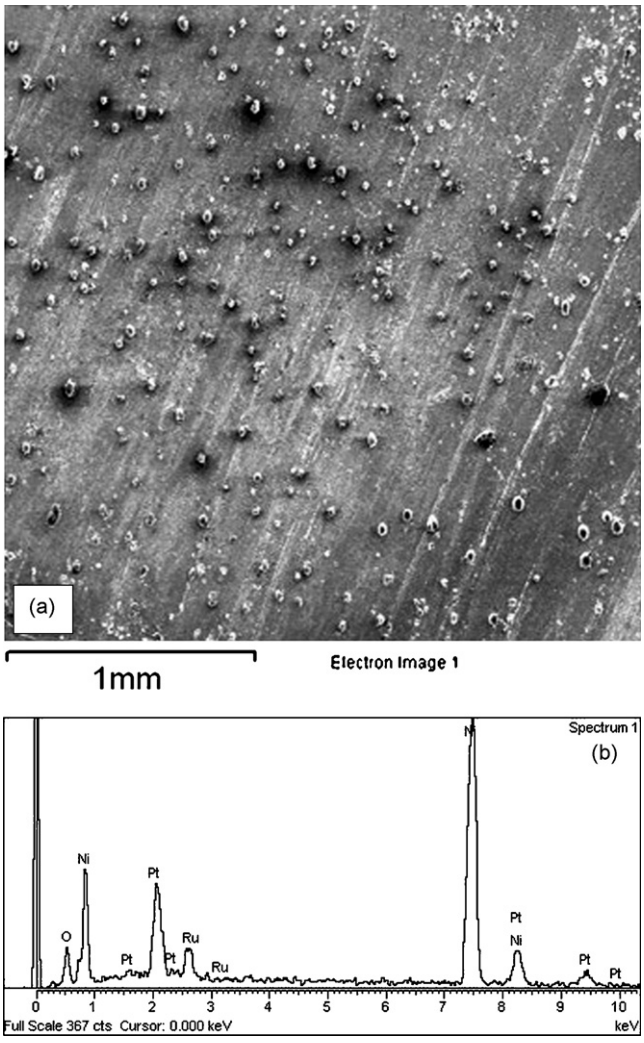

Fig. 1. (a) SEM image of Ni/Pt-Ru(2), 55 times magnified and (b) EDX spectrum of Ni/Pt-Ru(2).

3. Results and discussion

3.1. SEM-EDX analysis

Scanning electron microscopic (SEM) images of surfaces of Ni/Pt-Ru ($i = 1$–5) electrodes, their energy dispersion X-ray (EDX) spectra and tables for their composition, have been collected from the SEM-EDX study. A typical image, corresponding spectrum of Ni/Pt-Ru(2) electrode and a table for the compositions of all the electrodes from such spectra, are illustrated in Fig. 1a and b and Table 1, respectively. The magnification of images was 55 or 110 times in order to meet the requirement for getting an overall composition of an entire face of the two sides of the deposited foils. Since each of the two electrodes faces is equally preferred by the deposited ions, composition of one face is taken as the composition of the Pt-Ru composite deposit of the whole electrode surface. SEM images of all the electrodes show characteristic features of smooth black, grey and white portions associated with several white balls whose surroundings and sometimes centres are black in colour. Overall elemental surface compositions of all the electrodes, viz., Ni/Pt-Ru(i) have been obtained from all such EDX spectra and summarized in Table 1. The data reveal that Ni is present on the surface of the electrodes, mostly as metallic Ni(0) with some possible oxides of Ni as molecular oxygen cannot be present in the system. In fact, when white balls were analysed by EDX separately, it revealed that Ni was present there mostly as oxides of Ni, indicating a little chemical corrosion of Ni during deposition or latter. Moreover analysis of the different parts of white balls revealed that only the black centre of whole balls contained some Pt. Moreover, the large (6.62) at.% of Pt and only a small (0.81) at.% Ru were found in the black parts just beside the white balls. Thus overall analysis of SEM pictures (not shown) and the data of Table 1 lead us to conclude: (i) black portions and possibly some parts of grey portions are made of Pt and Pt-Ru deposits, (ii) Ru is mostly present outside the white balls and possibly rich in the green portions of the smooth surface, (iii) Ni is present mostly as metallic Ni surface outside the white balls, i.e., in the smooth portions; inside the white balls, Ni exists mostly as higher valent states, (iv) Pt is selectively more deposited just beside the white balls in addition to its co-deposition with Ru in the comparatively smooth surface of the electrode, (v) most of the areas of the surfaces of the electrodes do not contain any Pt-Ru deposit. Thus the overall electrode surface is composed of metallic Ni associated with nickel oxides/hydroxides, besides Pt and Ru electrocatalyst.

On increasing magnification of images to 40,000 times, corresponding to smooth portions of SEM images of one full side of planar electrode surface, we get highly magnified SEM images for all five Ni/Pt-Ru(i) electrodes studied. Three of them have been illustrated in Fig. 2a–c, respectively. The illustrations show black and white patches of various geometrical shapes of nanometer dimension. Thus in Fig. 2a, many black diffused rods are about 25–75 nm long and 2.5–5.0 nm in diameter. Similarly in Fig. 2b, two almost parallel rods are about 20 nm in length and 1.7–2.5 nm in diameter. In all these figures the diameter of disk-like patches are in the range of 2–3 nm. The diameters of circular white patches which may be oxides of Ru and Ni are also less than 5 nm. The excellent electrocatalytic activity of

Table 1
Elemental compositions of surface of Ni/Pt-Ru(i) ($i = 1$–5) electrodes, as obtained from EDX spectra

Element	Ni/Pt-Ru(1) (at.%)	Ni/Pt-Ru(2) (at.%)	Ni/Pt-Ru(3) (at.%)	Ni/Pt-Ru(4) (at.%)	Ni/Pt-Ru(5) (at.%)
O	19.42	18.86	17.67	15.80	15.21
Ni	72.36	72.75	72.95	78.81	82.67
Ru	1.40	2.71	3.88	2.61	1.28
Pt	6.82	5.68	5.51	2.78	0.84

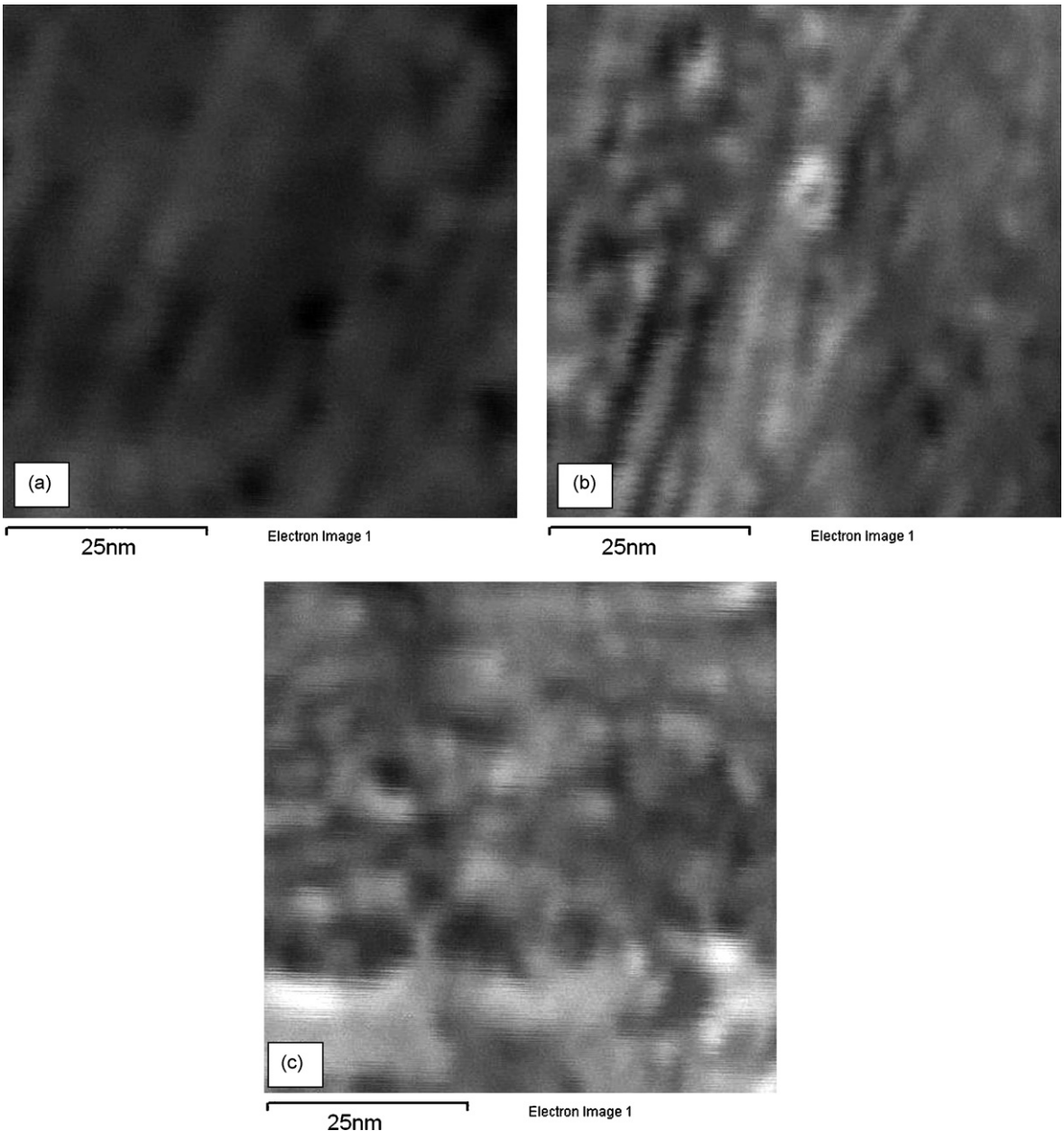

Fig. 2. SEM images of: (a) Ni/Pt-Ru(2), (b) Ni/Pt-Ru(3), (c) Ni/Pt-Ru(4) at 40,000 times magnification.

these electrodes, as it would be seen in the subsequent studies, is seemingly due to the presence of these crystallites of the deposit in nanometer scale, besides other factors.

3.1.1. Composition of Pt-Ru electrocatalyst on surface of electrodes

Relative elemental compositions of binary catalysts, viz., Pt and Ru in the deposition bath and in deposits on the surface of the electrodes, Ni/Pt-Ru(i) where $i = 1$–5, are presented in Table 2. The presence of other atoms (O, Ni) on the electrode surfaces and ions (H^+ Cl^-, etc.), molecules (H_2O, etc.) in solutions, have been ignored. For the bath solution the catalyst composition has been calculated from the known volume of two 2% (w/v) solutions mixed together, considering the presence of 40% (w/w) of metal in each precursor electrolyte as the specification. Notably, these compositions would be the catalyst compositions of the deposits of the different electrodes, had there been no difference in the susceptibilities of the metal ions to reduction. Actual catalyst compositions of the deposits of the different electrodes have also been presented in Table 2. They have been computed from the overall surface compositions of the electrodes, presented in Table 1 and obtained from the SEM study. The presence of other atoms except Pt-Ru atoms in the overall composition has been ignored to calculate the catalyst composition on surface of the electrodes. It is quite evident from the data presented in Table 2 that for all the electrodes of Ni/Pt-Ru(i) except when $i = 1$, Pt is deposited more and Ru is deposited less with respect to their composition in the bath solutions. This finding is however quite expected and hence the equilibrium potential of deposition of the two metals, which can be computed from the compositions of the

Table 2
Elemental catalyst composition in deposition bath and on surface of Ni/Pt-Ru(*i*) electrodes

Electrode	Possible elemental catalyst composition of binary Pt-Ru catalyst on the surface of the electrodes, as present in precursor electrolyte solution			Elemental catalyst composition of binary Pt-Ru catalyst on the surface of the electrodes as obtained from EDX study		
	Pt (at.%)	Ru (at.%)	Pt/Ru atom ratio	Pt (at.%)	Ru (at.%)	Pt/Ru atom ratio
Ni/Pt-Ru(1)	83.82	16.18	5.18	82.97	17.03	4.87
Ni/Pt-Ru(2)	63.33	36.67	1.73	67.74	32.26	2.10
Ni/Pt-Ru(3)	50.89	49.11	1.04	58.68	41.32	1.42
Ni/Pt-Ru(4)	42.53	57.47	0.74	51.58	48.42	1.07
Ni/Pt-Ru(5)	34.13	65.87	0.52	39.62	60.38	0.66

bath solutions. In the case of Ni/Pt-Ru(1), the relative amount of deposition of Pt and Ru, have been reversed, i.e., they become less and more, respectively, with respect to their composition in the bath solutions. This is possibly because when deposition of Pt is large, parallel hydrogen evolution during subsequent metal deposition may occur and hence hydrogen embrittlement [22,23] may cause for a decrease in at.% of Pt from the theoretical value as expected from the composition of the solution of the deposition bath. On the other hand, simultaneous deposition of Ru with Pt for all the electrodes and greater at.% of Ru in the deposit over that in bath solution in case of Ni/Pt-Ru(1) electrode, may be due to the ability of Ru to deposit on Pt by a phenomenon known as under potential deposition [24].

3.2. Cyclic voltammetric study

The cyclic voltammograms was taken in the range between −0.5 and 0.5 V since it had been reported that hydrogen adsorption/evolution appears below the range [21] and loss of Ru and Ni may occur above the range [25,26]. The voltammetric profiles resemble typical CV of alcohol oxidation in alkaline media, and shows both forward (i_F) and backward (i_B) current peaks in the anodic zone indicating simultaneous and consecutive steps of oxidation in the overall process. Fig. 3a depicts a typical system of cyclic voltammetric profiles which were obtained in 1 M NaOH without (blank) and with ethanol (1 M) for the latter's oxidation on Ni/Pt-Ru(3) electrode by application of consecutive triangular sweep of potential at the rate of 50 mv s^{-1}. It shows that on increasing the number of cycles, the anodic peak current density, i_F, increases with slight anodic shift of the peak potential E_F, until an apparent cyclic voltammetric steady state has been attained at about the 20–25th cycles. This seems to be due to creation of a little unblocked surface area by breakage of the M–OH bonds used for removal of carbonaceous intermediates on each cycling process until a steady state is reached. An increase of effective area on the surface of the electrodes helps to accumulate more carbonaceous poisonous intermediates on the surface during the next forward linear sweep of potential in the cycling process. The anodic shift of the peak potential (E_F) with an increase in the number of previous cycles, indicates more accumulation of such oxidative species which can be oxidized by the electrodes only at a higher potential. However, during the reverse scan of each cycle, viz., scan from +500 to −500 mV, a second anodic current peak (i_B) appears possibly due to the oxidation of all adsorbed carbonaceous species. In order to compare the electrocatalytic capabilities of all five electrodes studied, all the steady CV after repeated cycling are presented in Fig. 3b. It is quite apparent from the figure that i_B is greater for an electrode where i_F is greater. In fact for all these electrodes i_B follows a linear relationship with i_F (Fig. 3c), indicating that greater the dehydrogenation in the forward scan, the greater is the accumulation of carbonaceous poisons, as observed by i_B during reverse scanning. Plots of i_F and i_B with at.% of Ru indicate that the maxima of the profiles were at 40% Ru as can be observed from Fig. 3c. Among the electrodes studied, the best electrode is Ni/Pt-Ru(3). Thus the electrode containing 40% Ru is the best among the electrodes studied. It has been pointed out that the tolerance power towards carbonaceous poisons may be measured [27] by i_F/i_B. It represents the capability of an electrode to oxidize the poisons at the potential where dehydrogenation occurs. Here, this ratio is above 2, i.e., quite large as compared to that of other electrodes that are available in the literature [1,27–31]. However, when i_F/i_B is plotted against % composition of Ru (Fig. 3e), it has been found that the least value of the ratio is obtained for Ni/Pt-Ru(3) electrode, where maximum peak current density is obtained. This is seemingly due to the fact that the rate of formation of Pt–CH_3 intermediate is greater for the electrodes where peak current density is larger and so CH_4 eliminates from those systems following the chemical reaction:

$$\text{Pt–CH}_3 + \text{Pt–H} = 2\text{Pt} + \text{CH}_4 \quad (2)$$

which is in conformation with the mechanism proposed by several studies [1,27]. Thus if Pt–CH_3 is removed as CH_4 instead of being completely oxidized to CO_2 and H_2O following possible electrochemical reaction:

$$\text{Pt–CH}_3 + 2\text{RuOH} = \text{Pt} + \text{CO}_2 + 2\text{Ru} + 5\text{H}^+ + 5\text{e} \quad (3)$$

loss in i_F which is mainly developed for dehydrogenation reaction, is comparatively more than that of i_B, which is mainly arisen for the oxidation of carbonaceous poisons. Thus i_F/i_B is the least for the best of the electrodes studied here.

3.3. Chronopotentiometric study

Fig. 4a shows the variation of potential with time on application of a relatively large constant current density of 0.4 mA cm^{-2}. Three characteristic potential regions are observed in transition from a lower potential region to a higher

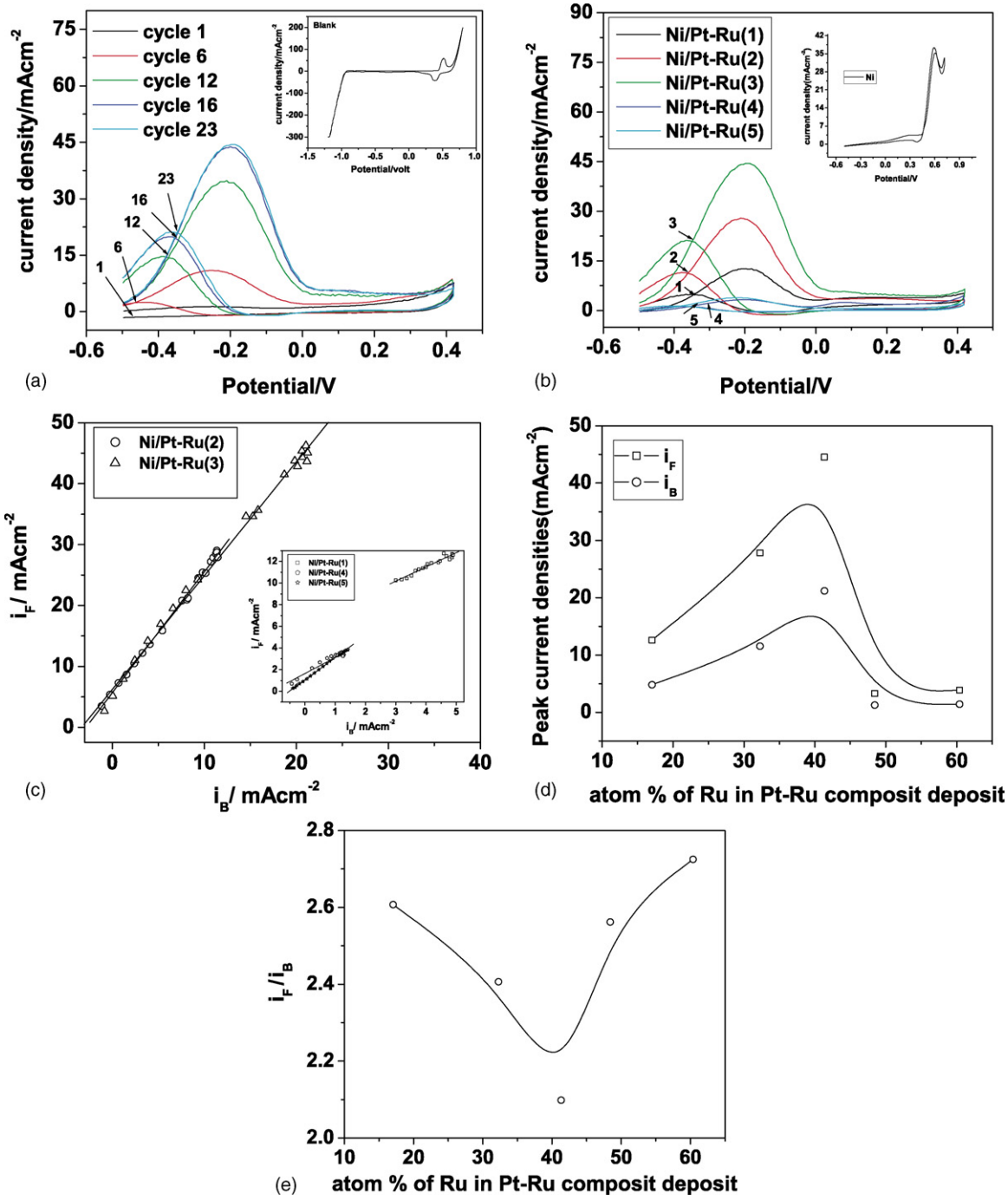

Fig. 3. (a) Cyclic voltammograms for ethanol oxidation in 1 M ethanolic solution of 1 M NaOH on Ni/Pt-Ru(3), the profile with 1 M NaOH being shown in the inset, (b) cyclic voltammograms of steady cycles of Ni/Pt-Ru(*i*) and bare Ni foil (inset), (c) a linear plot of i_F vs. i_B of the five electrodes, (d) a plot of peak current densities vs. atomic percentage of Ru in Pt-Ru deposit, (e) a plot of (i_F/i_B) vs. atomic percentage of Ru in Pt-Ru deposit.

potential zone in each of these profiles. In the lower potential region (−0.5 to −0.3 V), potential rises slowly with time. It signifies activation controlled simultaneous dehydrogenation and decarbonaceous oxidation of ethanol, as substantiated by the lower potential formation of M–H bond by mainly Pt with C_2H_5OH and of M–OH bonds by Ru and Ni with H_2O as observed by others [6,26]. A gradual increase of potential in this region seemingly indicates relatively faster rate of dehydrogenation of alcohols than rate of oxidation of carbonaceous species with net result of gradual accumulation of carbonaceous poisons which need higher potential for complete oxidation. The potential in the middle potential region (−0.3 to 0.4 V) however rises very steeply with time, indicating that surface covered by carbonaceous poison is so large in this region that the contribution by carbonaceous oxidation to the overall galvanostatic current is fast becoming nearly the same as that contributed by the dehydrogenation and that the scope for dehydrogenation is gradually becoming insignificant due to lack of free surface for ethanol

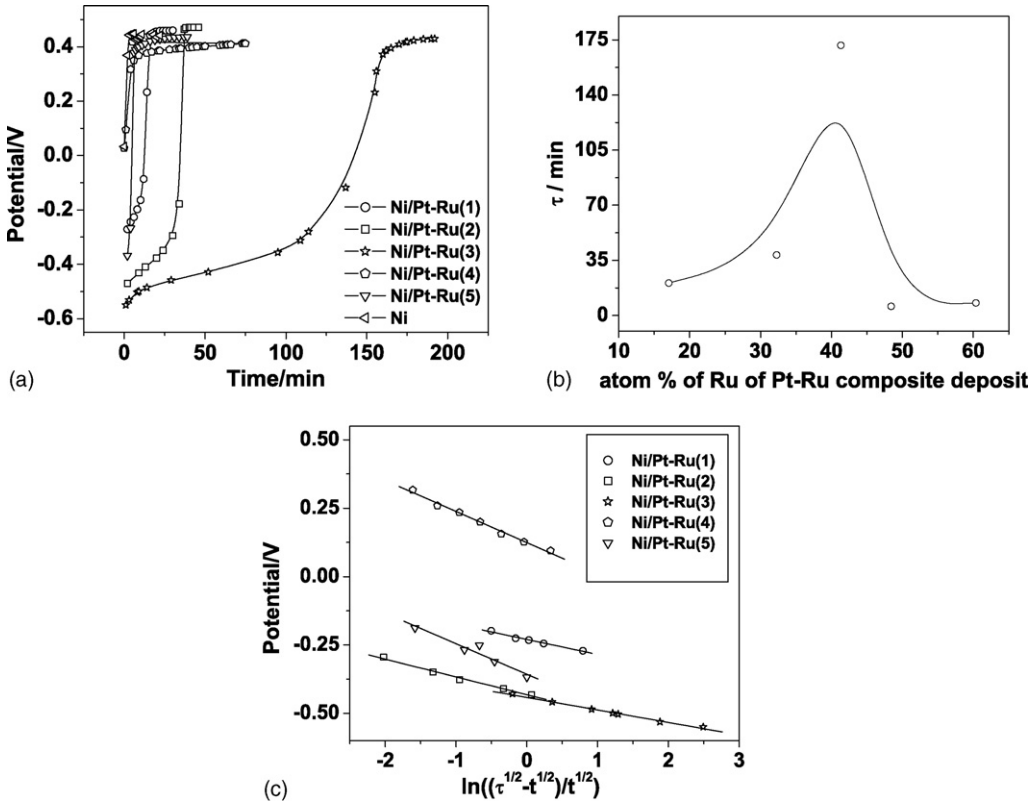

Fig. 4. (a) Chronopotentiometric potential–time profile for ethanol oxidation on bare Ni foil and different Ni/Pt-Ru(*i*) electrodes immersed in 1 M ethanolic solution of 1 M NaOH, (b) a plot of τ vs. atomic percentage of Ru in Pt-Ru deposition different electrodes of Ni/Pt-Ru(*i*), (c) plot of potential vs. $\left[\ln\left((\tau^{1/2} - t^{1/2})/t^{1/2}\right)\right]$ for different Ni/Pt-Ru(*i*) electrodes studied in 1 M ethanolic solution of 1 M NaOH.

adsorption. The region above 0.4 V signifies probably an attainment of steady state for oxidation on Pt and Ru. Notably, above 0.45 V, as it has been shown from CV study (Fig. 3a), would be seen from Tafel plots (Fig. 5a) in the next section, oxidation of NiO to NiOOH and ethanol oxidation on them, takes place in conformation with other studies [20]. However, on comparison of the chronopotentiometric profiles, they reveal that at any instant the potential requirement for drawing a particular current from the system and the 'onset' potential of the anode varies in the order: Ni/Pt-Ru(5) > Ni/Pt-Ru(4) > Ni/Pt-Ru(1) > Ni/Pt-Ru(2) > Ni/Pt-Ru(3), reflecting an exactly reverse order of electrocatalytic capability. In other words, Ni/Pt-Ru(3) provides the maximum resistance towards electrode poisoning and Ni/Pt-Ru(5) provides the minimum. Moreover detailed analysis of chronopotentiometric profiles, reveal that the transition time, τ increases in the order: Ni/Pt-Ru(5) < Ni/Pt-Ru(4) < Ni/Pt-Ru(1) < Ni/Pt-Ru(2) < Ni/Pt-Ru(3) with an indication of the resistance offered by different types of electrodes towards poisoning. In Fig. 4b, τ has been plotted against composition (at.% Ru) of the composite deposit and the profile reflects 40% Ru is the best resistor for poisoning among the electrodes studied. A further analysis of chronopotentiometric profiles reveal straight line plots of observed potential, E versus $\ln(\tau^{1/2} - t^{1/2})/t^{1/2}$, conforming to equation:

$$E = E' - \frac{RT}{\alpha n_a F} \ln \frac{\tau^{1/2} - t^{1/2}}{t^{1/2}} \quad (4)$$

where the terms bear the usual significances [30].

These plots are shown in Fig. 4c.

The lower slope of an electrode reflects greater αn_a (=transmission co-efficient × number of electrons transferred) and hence better electrocatalytic activity for the electrode than that for an electrode possessing higher slope. On the other hand, the higher negative potential of the intercept E' indicates more powerful intrinsic catalytic [21] nature of the electrode as compared to one possessing lower negative intercept E'. The intercept values (in volts) given in parentheses, signify the intrinsic catalytic power of the electrodes and are as follows:

Ni/Pt-Ru(3)[−0.4418]

> Ni/Pt-Ru(2)[−0.4318] > Ni/Pt-Ru(5)[−0.3570]

> Ni/Pt-Ru(1)[−0.2298] > Ni/Pt-Ru(4)[0.1242]

3.4. Steady state polarization

Steady state galvanostatic polarization study at relatively higher potentials was performed for all the electrodes of Ni/Pt-Ru systems in 1 M ethanolic solution of 1 M NaOH. The study was made in order to compare the electrocatalytic activity of the working anodes at higher potentials. For this, the current density applied was in the range between 0.2 and 3.2 mA cm^{-2}. These current densities ensure maximum value of steady state potential to be 0.48 V. This potential is however below the potential for Ni(II) → Ni(III) formation in presence of ethanol [28]. Notably, it has been reported that above this potential, a conversion of NiO

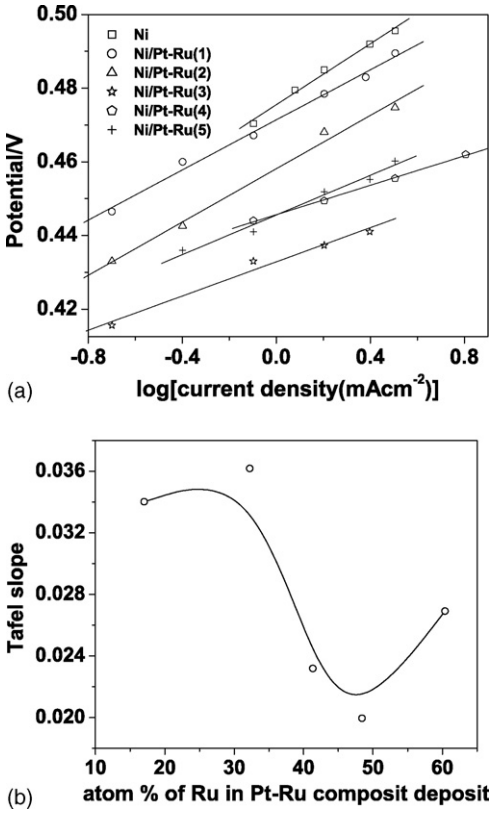

Fig. 5. (a) Plot of steady state potential vs. log (current density (mA cm^{-2})) for different Ni/Pt-Ru(*i*) electrodes and bare Ni electrode immersed in 1 M ethanolic solution of 1 M NaOH and (b) plot of Tafel slope vs. atomic percentage of Ru in Pt-Ru deposit on Ni support.

to NiO(OH) takes place in 1 M NaOH, in absence of ethanol. But as evident from our cyclic voltammetric studies [21] and works of others [28], such oxidation does not occur in this potential in alkaline solution, in presence of ethanol. So the result possibly reflects the true electrocatalytic power of the system of Ni/Pt-Ru electrodes for ethanol oxidation. Fig. 5a illustrates the Tafel plots for anodic oxidation of ethanol on all the Pt-Ru coated anodes studied at room temperature. The curves follow linear Tafel relation according to the equation:

$$E = E_e - \frac{2.303RT}{\alpha nF}\log i_0 + \frac{2.303RT}{\alpha nF}\log i \quad (5)$$

upto a potential of about 0.5 V. Fig. 5a reveals that for drawing any fixed current density from the system within the range of 0.2–3.2 mA cm^{-2}, the potential requirement of the anode varies in the order: Ni > Ni/Pt-Ru(1) > Ni/Pt-Ru(2) > Ni/Pt-Ru(5) > Ni/Pt-Ru(4) > Ni/Pt-Ru(3) reflecting an exactly reverse order of electrocatalytic capability at relatively high potential. The same result is also observed from the Tafel slopes which are 0.0582, 0.034, 0.036, 0.023, 0.020 and 0.027 V for Ni, Ni/Pt-Ru(1), (2), (3), (4) and (5) electrodes, respectively. The order of intercepts (values shown in brackets) are Ni/Pt-Ru(1)(0.471 V) > Ni/Pt-Ru(2)(0.458 V) > Ni/Pt-Ru(4)(0.446 V) > Ni/Pt-Ru(5)(0.445 V) > Ni/Pt-Ru(3)(0.433 V), indicating possibility of greater equilibrium exchange current density, i_o, for Ni/Pt-Ru(3) electrode than that of other electrodes studied.

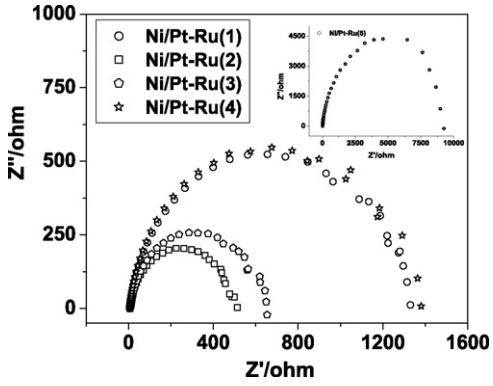

Fig. 6. Electrochemical impedance spectra in 1 M ethanolic solution of 1 M NaOH at −0.5 V w.r.t. MMO on Ni/Pt-Ru(*i*).

In Fig. 5b, plot of Tafel slope versus at.% of Ru shows that 47 at.% Ru in Pt-Ru mixture, is the best composition among the electrode-catalyst studied. This result is also consistent with CV and chronopotentiometric studies.

3.5. Electrochemical impedance spectroscopy

Semicircular Nyquist plots of imaginary (Z'' (Ω)) versus real (Z' (Ω)) components of impedance for ethanol oxidation in 1 M ethanolic solution of 1 M NaOH on different Ni/Pt-Ru(*i*) electrodes of various composition, are presented in Fig. 6. The illustrations are shown at only one potential in the lower potential region, viz., at −0.5 V with respect to MMO. Semicircular plots indicate kinetically controlled reactions. It is well known that a decrease in charge transfer resistance, R_{ct}, as obtained from diameter of the semicircular Nyquist plot, and signifies an enhancement of the charge transfer kinetics. In fact, at potentials near equilibrium regions, R_{ct} can be related with the equilibrium exchange current density (i_o) by the following equation [32]:

$$R_{ct} = \frac{RT}{nFAi_o} \quad (6)$$

where $i_0 = nFK_oC_o^{1-\alpha}C_R^{\alpha}/A$, R is the molar gas constant (J mol^{-1} K^{-1}), T the temperature (K), n the number of electrons transferred, F Faraday constant (coulomb), A the area of electrode (cm^{-2}), K_o the standard heterogeneous rate constant, C_o, C_R the bulk concentrations of oxidants and reductants (mol L^{-1}) and α is the transfer co-efficient. Since C_o, C_R and A were kept constant for all the electrodes studied, R_{ct} values of the electrodes are amenable to comparison, in reference to the electrocatalytic activity of the electrodes. From Table 3, it is evident that charge transfer conductance per unit area, $1/AR_{ct}$ and hence electrocatalytic activity of the electrodes varies in the order Ni/Pt-Ru(2) > Ni/Pt-Ru(3) > Ni/Pt-Ru(1) > Ni/Pt-Ru(4) > Ni/Pt-Ru(5), at lower equilibrium region. This order of electrocatalytic activity at near equilibrium region however differs to some extent from that obtained from the studies like GP, CP and CV. In the present study, Ni/Pt-Ru(2) seems to be better than Ni/Pt-Ru(3) electrode, whereas from other studies we find the latter is better. This is possibly due to the fact that GP and CP studies were done at conditions of high current drag and hence

Table 3
Variation of charge transfer resistance for oxidation of ethanol with composition (at.%) of Ni/Pt-Ru(i) electrodes studied

Electrode	Area of the electrodes studied (cm^2)	% of Ru	R_{ct} at −500 mV	Charge transfer conductance per unit area, $1/AR_{ct}$ ($\Omega^{-1}\,cm^{-2}$)
Ni/Pt-Ru(1)	0.0581	17.03	1327.43	0.0130
Ni/Pt-Ru(2)	0.0475	32.26	515.60	0.0408
Ni/Pt-Ru(3)	0.0475	41.32	652.74	0.0322
Ni/Pt-Ru(4)	0.0581	48.42	1382.78	0.0124
Ni/Pt-Ru(5)	0.0475	60.38	9285.28	0.0023

of high potentials. CV study was also done as usual for oxidation from low potential to high potential region where diffusion superimposes on activation kinetics. So the outcome of EIS study which was performed at lower potential differs slightly from the former studies, done at relatively higher potentials. Notably, the requirement of Ru content is less at lower potential for the best performance of the electrode.

4. Conclusion

This study concludes that 32–47 at.% of Ru is the best range of composition for high catalytic power from a Pt-Ru binary electrocatalyst deposited on a Ni-support, at least for the described construction procedure for these electrodes. For drawing a large current density or for higher potentials, anodes with a Pt-Ru electrocatalyst containing 39–47 at.% of Ru is favoured, as evident from the CV, chronopotentiometric and galvanostatic polarization studies. On the other hand, the electrocatalyst containing 32–36 at.% of Ru on a Ni support is favoured when the current drawn is lower or the potential applied is nearer to the equilibrium potential, as evident from the EIS study. The excellent electrocatalytic behaviour of these electrodes is possibly due to not only the composition but also the formation of well dispersed nano-sized patches of the Pt-Ru deposit with different geometrical shapes including rods, disks, etc., as evident from SEM study. The electrocatalytic capability of the support, i.e., the planar Ni surface, may also have a definite role, as another oxophilic element like Ru, to remove the catalytic poisons but at high potentials. Of course, our conclusions are based on the consideration of not too much difference in the shape and size of the deposit patches of the composite electrocatalyst, as evident from the SEM study. However more firm and stringent conclusions can be derived only if electrodes are prepared with electrocatalyst particles of nanometer dimensions and with an even distribution, which are no doubt very difficult to control and characterize on a solid surface.

It is noteworthy in this study, that although most of the surface of the electrodes is not fully covered with the catalyst-deposit as evident from SEM study, the catalytic capability of the constructed electrodes is excellent.

Acknowledgments

We gratefully acknowledge financial assistance from University with Potential for Excellence of the UGC, New Delhi, Scheme (Rec/N/66/04).

Help of Professor J. Datta and Shri S. Sengupta of Department of Chemistry, BESU, Howrah, India to take EIS data from their laboratory is also acknowledged.

References

[1] C. Lamy, A. Lima, V. Le Rhun, F. Delime, C. Coutanceau, J.-M. Leger, J. Power Sources 105 (2002) 283.
[2] M. Watanabe, S. Motoo, J. Electroanal. Interfacial Electrochem. 60 (1975) 267.
[3] S. Katsuaki, I. Ryuhei, K. Hideaki, J. Electroanal. Chem. 284 (1990) 523.
[4] Z. Jusys, T.J. Schmidt, L. Dubau, K. Lasch, L. Jorissen, L. Garche, R.J. Behm, J. Power Sources 105 (2002) 297.
[5] (a) S. Sengupta, J. Datta, J. Power Sources 145 (2005) 124;
(b) S. Sengupta, S.S. Mahapatra, J. Datta, J. Power Sources 131 (2004) 169.
[6] H.H. Zhou, X.H. Ning, J.H. Chen, W.Z. Wei, Y.F. Kuang, Ind. J. Chem. 44A (2005) 1009.
[7] A. Kabbabi, R. Faure, R. Durand, B. Beden, F. Hahn, M. Leger, C. Lamy, J. Electroanal. Chem. 444 (1998) 41.
[8] A. Chrzanowski, A. Wieckowski, Langmuir 14 (1998) 1967.
[9] L. Dubau, C. Coutanceau, E. Gornier, J.M. Leger, C. Lamy, J. Appl. Electrochem. 33 (2003) 419.
[10] H.A. Gasteiger, N. Markovic, P.N. Ross Jr., J. Cairns Elton, J. Phys. Chem. 97 (1993) 12020.
[11] D. Chu, S. Gilman, J. Electrochem. Soc. 143 (5) (1996) 1685.
[12] H.N. Dinh, X. Ren, F.H. Garzon, P. Zelenay, S. Gottesfeld, J. Electroanal. Chem. 491 (2000) 222.
[13] M. Watanabe, M. Uchida, S. Motoo, J. Electroanal. Chem. 229 (1987) 395.
[14] H.A. Gasteiger, N. Markovic, P.N. Ross Jr., J. Cairns Elton, J. Phys. Chem. 98 (1994) 617.
[15] T. Iwasita, H. Hoster, A. John-Anaeker, W.F. Lin, W. Vielstich, Langmuir 16 (2) (2000) 522.
[16] H. Hoster, T. Iwasita, B. Hermann, Vielstich Wolf, Phy. Chem. Chem. Phys. 3 (2001) 337.
[17] D.R. Lide (Ed.), Hand Book of Chemistry & Physics, 83rd ed., CRC, LLC, 2002–2003.
[18] K. Nishimura, K. Machida, M. Enyo, J. Electroanal. Chem. 251 (1998) 117.
[19] R. Parsons, N.T. Vander, J. Electroanal. Chem. 257 (1998) 9.
[20] M.A. Abdel Rahim, R.M. Abdel Hameed, M.W. Khalil, J. Power Sources 134 (2004) 160.
[21] P. Paul, J. Bagchi, S.K. Bhattacharya, Ind. J. Chem. (A) (2006).
[22] M.C. Fallis, M.S. Daw, C.Y. Fong, Phys. Rev. B 51 (1995) 7817.
[23] A.F. Wright, A.F. Daw, C.Y. Fong, Atomic Scale Calculations of Structure in Materials, MRS, Pittsburg, 1990.
[24] D. Colle Vinicius, G.M. Janete, T. Filho Germano, J. Braz. Chem. Soc. 14 (4) (2003) 601.
[25] J.-W. Kim, S.-M. Park, J. Electrochem. Soc. 146 (3) (1999) 1075.

[26] K.W. Park, J.H. Choi, B.K. Kwon, S.A. Lee, Y.E. Sung, H.Y. Ha, S.A. Hong, H. Kim, A. Wieckowski, J. Phys. Chem. B 106 (2002) 1869.
[27] Z. Liu, X. Yi Ling, X. Su, J.Y. Lee, L.M. Gan, J. Power Sources 149 (2005) 1.
[28] A.O. Neto, J. Perez, W.T. Napporn, E.A. Napporn, E.A. Ticlanelli, E.R. Gonzalez, J. Braz. Chem. Soc. 11 (2000) 39.
[29] T. Frelink, W. Visscher, J.A.R. Van Veen, Electrochim. Acta 40 (1995) 1537.
[30] M. Enyo, J. Appl. Electrochem. 15 (1985) 907.
[31] D.F.A. Koch, D.A.G. Rand, R. Woods, J. Electroanal. Chem. 70 (1976) 73.
[32] A.J. Bard, Faulkner, Electrochemical Methods, John Wiley & Sons, 1980.